Simulations evidencing two surface tensions for fluids confined in nanopores

H.R. Jiang, S.L. Zhao, W. Dong

Simulations evidencing two surface tensions for fluids confined in nanopores

H. R. Jiang [1, 2], S. L. Zhao [1, 3, *] and W. Dong [2, *]

[1] *State Key Laboratory of Chemical Engineering and School of Chemical Engineering, East China University of Science and Technology, 200237 Shanghai, China*

[2] *Laboratoire de Chimie, Ecole Normale Supérieure de Lyon, UMR 5182, CNRS, 46, Allée d'Italie, 69364 Lyon Cedex 07, France*

[3] *State Key Laboratory of Featured Metal Materials and Life-cycle Safety for Composite Structures, and School of Chemistry and Chemical Engineering, Guangxi University, Nanning 530004, China*

As first recognized by Hill in 1960's, one character distinguishing the thermodynamics of small systems from the macroscopic one is that some intensive variables are no longer defined uniquely for small systems. For example, the differential chemical potential, defined as the derivative of a thermodynamic potential with respect to particle number, is no longer equal to the integral one, given by the ratio of Gibbs free energy to the particle number. The concept of differential and integral surface tensions has been introduced recently to account for the increasing surface contribution to thermodynamic potentials when a system shrinks down in size. Simulations constitute a powerful tool for testing new concepts. The present work provides the simulation evidence for distinct differential and integral surface tensions. Our results point out some useful directions for future experimental investigations to check the general validity of the concept of differential and integral surface tensions.

[*] Emails: szhao@gxu.edu.cn, wei.dong@ens-lyon.fr

I. Introduction

Thermodynamics provides a powerful framework for many scientific domains and technological applications. It was primarily developed for describing macroscopic systems. T. L. Hill was a pioneer who had proposed extending thermodynamics to small systems in 1960s by introducing an additional pair of conjugated variables, i.e., replica number and subdivision potential [1,2]. Until now, none of these two variables has been determined experimentally. The lack of experimental validation constitutes a major obstacle for the wide acceptation of Hill's theory, now named as nanothermodynamics [3-5]. However, it is attracting much renewed interest [5-21] due to the booming nanotechnology. Recently, an alternative approach has been proposed for extending thermodynamics down to nanoscales without resorting to Hill's replica trick but by focusing on a single small system and by introducing the new concept of differential and integral surface tensions, which are, in principle, both experimentally measurable quantities [22,23].

Surface tension is a venerable scientific concept, Laplace [24] and Young [25] initiated its study to understand capillarity. Gibbs introduced its thermodynamic definition and derived its relation to the adsorption at surfaces or interfaces [26]. The statistical-mechanics expression of the surface tension and that of pressure tensor were derived by Kirkwood and coworkers from their respective mechanical definition [27,28], (see also refs [29, 30] for reviews). Many simulation methods are now available for calculating the surface tensions of various interfaces [31-47] (the cited references not intending to be exhaustive). Experimental evidences start appearing to show the importance of surface contribution to thermodynamic potentials of nanoscale systems [48,49]. It has been revealed recently that when the surface contribution becomes dominant to a system's thermodynamic potential, two distinct surface tensions can arise, i.e., one named as differential surface tension, defined as the derivative of a thermodynamic potential with respect to interface area, and the other named as integral surface tension, given by the excess thermodynamic potential divided by surface area (see Eqs. 2 - 4 for more precise definitions) [22,23]. Fig. 1 shows a prototype of such interfacial systems, e.g., a hard sphere fluid confined in a slit pore between two flat hard walls (model studied in this work). This is a benchmark model for the study of confined fluids and many theoretical and simulation works have been devoted to it. Despite our extensive literature search, we have not found any previous work giving whatever indication that the differential and integral definitions of surface tension can give different results. So, there is an obvious gap between the recent prediction of two distinct surface tensions [22,23] and the currently

available experimental and simulation data. The primary objective of the present work is for bridging this gap, at least that between the recent theoretical prediction and the previous simulations, i.e., evidencing the general validity of the concept of differential and integral surface tensions through detailed simulations. We believe that the feasibility demonstration and the search of optimal experimental conditions are really necessary and very valuable for motivating the endeavor devoted to

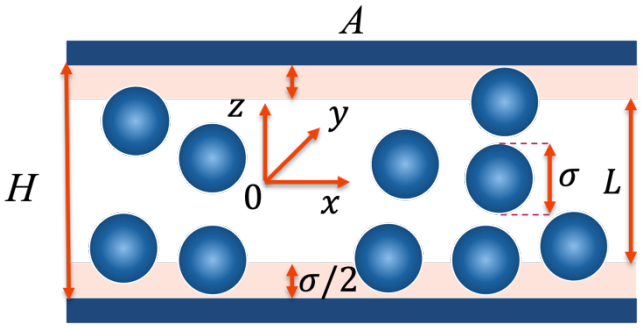

FIG.1 A hard sphere (HS) fluid, of diameter σ, confined in a slit pore formed by two hard walls. Pore width: H (accessible pore width: $L = H - \sigma$); Surface area of one wall: A (total surface area: $\mathcal{A} = 2A$).

the experimental validation. Before engaging actively in such an endeavor, any experimental group can raise the following relevant and important questions. At which pore sizes (e.g., in terms of fluid-particle diameter), the distinct differential and integral surface tensions can show up? What should be the magnitude of the difference between the differential and integral surface tensions? Is the difference sufficiently large to be experimentally detectable? The present work aims at bringing some answers to these questions. The previous theoretical prediction of the two distinct surface tensions was based on a model with an ideal gas, which does not allow for answering many questions raised above. For example, the ideal gas is constituted of point particles, so no volume exclusion effect between fluid particles is taken into account. However, it is well-known that the repulsion between fluid particles at short distances is mainly responsible for the short-range structure in any real bulk and confined fluids. We believe that today, sixty years after Hill's first work on thermodynamics of small systems, any efforts devoted to evidence the hallmark thermodynamic behaviors of small systems are worthwhile and timely endeavors. From a broader perspective, the firm establishment of distinct differential and integral intensive thermodynamic variables will advance our general understanding of thermodynamics. In the framework of macroscopic thermodynamics, the intensive variables, like pressure and chemical potential, play an important role for charactering thermodynamic equilibrium.

For the moment, it is not yet clear whether it is the differential or the integral intensive variable that enters into the conditions for determining the equilibrium in a nanoscale system. We believe such open questions will become interesting future research issues.

From its mechanical definition, the surface tension is given by,

$$\gamma^{\mathrm{mech}} = \frac{1}{2}\int_{-L/2}^{L/2} dz[p_{\perp} - p_{\parallel}(z)] \ , \tag{1}$$

where $p_{\perp}$ and $p_{\parallel}(z)$ are respectively the normal and transverse component of the pressure tensor and the factor $1/2$ accounts for the two fluid-wall interfaces. One well-known thermodynamic definition gives,

$$\gamma = \left(\frac{\partial F}{\partial \mathcal{A}}\right)_{T,V,N} = \left(\frac{\partial \Omega}{\partial \mathcal{A}}\right)_{T,V,\mu} = \left(\frac{\partial G}{\partial \mathcal{A}}\right)_{T,p_{\perp},N} \ , \tag{2}$$

where F , G, and Ω are respectively the Helmholtz, Gibbs free energy and the grand potential of the confined fluid, V, N, T and μ are respectively volume, number of particles, temperature and chemical potential. Although the definitions given in eqs. (1) and (2) should be considered now as the standard knowledge of surface thermodynamics, their precise meaning and their relations are not always clearly perceived, thus they are considered sometimes as different things. When the expressions of $p_{\perp}$ and $p_{\parallel}(z)$ derived by Ivring and Kirkwood [28] are substituted into eq. (1), one obtains an expression of γ^{mech} in terms of fluid-fluid and fluid-wall interactions. Starting from eq. (2) with a chosen thermodynamic potential and its corresponding partition function and taking properly the derivative with respect to surface area, Dong, Franosch, Shilling [55] have shown recently that eq. (2) gives exactly the same result as eq. (1). This shows clearly that the mechanical definition is identical to the differential thermodynamic definition of surface tension, as already pointed out in some particular cases [22,23]. The equivalence of the definitions given in eqs. (1) and (2) allows for calculating the differential surface tension from either of them.

Gibbs [26] and Cahn [50] gave respectively also the following expressions of surface tension,

$$\hat{\gamma}_{\Omega} = \frac{\Omega(T,\mu,V,\mathcal{A}) - \Omega^{\mathrm{bulk}}}{\mathcal{A}} = \frac{\Omega(T,\mu,V,\mathcal{A}) + p^{\mathrm{bulk}}V}{\mathcal{A}} \ , \tag{3}$$

$$\hat{\gamma}_{G} = \frac{G(T,p,N,\mathcal{A}) - G^{\mathrm{bulk}}}{\mathcal{A}} = \frac{G(T,p,N,\mathcal{A}) - \mu^{\mathrm{bulk}}N}{\mathcal{A}} \ , \tag{4}$$

where Ω^{bulk} and G^{bulk} are respectively the grand potential and the Gibbs free energy of the considered fluid in bulk. While eq. (2) gives the surface tension from the derivative of a thermodynamic potential, the ones defined by eqs. (3) and (4) are based on finite differences. So, the former has been named recently as differential surface tension while the latter as integral surface

tension [22,23]. When the pore width is large, all the above expressions give the same result. In fact, all the previous simulations for determining the surface tension have been carried out under such conditions. With the help of the model of a strongly confined ideal gas [22,23], a prediction has been made recently: the differential and integral surface tensions are no longer the same. Moreover, the integral surface tensions can be ensemble-dependent, e.g., eqs. (3) and (4) give different results, while the differential surface tension is ensemble-independent, i.e., eq. (2) holds even when the slit pore becomes very narrow. Thus, it is necessary to indicate which thermodynamic potential is used to define an integral surface tension. The index used for an integral surface tension serves for this purpose, e.g., $\hat{\gamma}_{\Omega}$ and $\hat{\gamma}_{G}$. In order to motivate experimental groups to engage actively in the investigations devoted to test the predictions of nanoscale thermodynamics, it is necessary to go beyond the ideal gas model since some key questions concerning the experimental feasibility and the detection conditions can not be answered with the ideal-gas model constituted of point particles. An immediate such question is: for which pore sizes (in terms of fluid-particle diameter) one can expect to see distinct differential and integral surface tensions?

It is true that the system chosen for the present study, i.e., a hard-sphere fluid in a slit pore, is still a simplified model for fluids. However, it is capable of capturing some key general features of real fluids. For example, the structure factor of some simple liquids determined from neutron-scattering experiments is quite close to that given by a HS model. Moreover, the HS model can account for a large part of a fluid's free energy since it is a well-known good reference system widely used in perturbation theories for describing real fluids. Since it is no longer possible to obtain exact and analytical results for a HS fluid confined in a slit pore, we resort to computer simulations in the present work.

II. Methods

A. Calculation of integral surface tension, $\hat{\gamma}_{\Omega}$

The most straightforward way to determine the integral surface tension in a grand canonical ensemble, i.e., $\hat{\gamma}_{\Omega}$ is to use its definition given in eq. (3). The grand potential of the confined fluid can be obtained by using the Grand Canonical Transition Matrix Monte Carlo method (GCTMMC) proposed by Errington [51,52]. To determine the grand potential of the bulk fluid, we use Carnahan-Stirling equation to calculate the pressure of the bulk hard sphere fluid in chemical equilibrium with the confined fluid. To apply eq. (3), we need to choose also the reference surfaces with respect to which the surface tension

is calculated. In the present work, all the results are obtained by choosing the reference surfaces at $z = \pm L/2$ (see Fig. 1), thus, $V = LA$ (A: surface area of one wall).

It is also possible to calculate $\hat{\gamma}_\Omega$ by integrating Gibbs adsorption equation, i.e.,

$$\left(\frac{\partial \hat{\gamma}_\Omega}{\partial \mu}\right)_{T,L} = -\Gamma = -\frac{N - N^{\text{bulk}}}{\mathcal{A}} \quad , \tag{5}$$

where Γ is the adsorption and N^{bulk} the number of the corresponding bulk fluid at the same T, the same μ and occupying a volume in the bulk equal to that of the confined fluid. This method, named as Gibbs-Cahn integration, has been successfully explored by B. B. Laird and coworkers for calculating surface tension at a single interface [46]. In the present work, we do not use this method since it requires calculating a series of values of the adsorption as well as the determination of the integration constant, i.e., one value of the surface tension by using another method. However, it is to be pointed out that this method can provide a useful basis for the experimental determination of $\hat{\gamma}_\Omega$ since the experimental measurement of the adsorption is a routine one.

B. Calculation of differential surface tension, γ

As already pointed out above, the mechanical definition of surface tension, i.e., eq. (1), is identical to the thermodynamic differential definition given in eq. (2). Moreover, it has been shown that the differential surface tension is ensemble-independent [22,23]. So, eq. (1) can be used with any ensemble provided one chooses the corresponding thermodynamic potential to calculate γ as required by eq. (2). Eq. (2) shows that the differential surface tension can be calculated by taking the derivative of the grand potential with respect to surface area when the grand-canonical ensemble is considered. Nevertheless, a simpler alternative way to calculate the differential surface tension exists by exploring the fact that the grand potential is a first-order homogeneous function of both V and $\mathcal{A}$. For a given finite pore width, the volume of the slit pore scales with the pore surface area [22], i.e.,

$$\Omega(T, \mu, \lambda V, \lambda \mathcal{A}) = \lambda \Omega(T, \mu, V, \mathcal{A}) \quad . \tag{6}$$

This leads immediately to

$$\Omega(T, \mu, V, \mathcal{A}) = -p_\perp V + \gamma \mathcal{A} \quad . \tag{7}$$

In contrast to eq .(3), γ in eq.(7) is the differential surface tension while $\hat{\gamma}_\Omega$ in eq.(3) is the integral surface tension since p^{bulk} in eq.(3) is the pressure in the reservoir of the grand canonical ensemble while $p_\perp$ in eq.(7) is the normal pressure of the confined fluid on the pore walls. When these two pressures are not equal, their difference, $\Pi = p_\perp - p^{\text{bulk}}$, is Derjaguin's disjoining pressure [53,54]. Dong, Franosch and Schilling have proven recently that the contact-value theorem holds also for a

hard sphere fluid confined in a hard slit pore for any pore width [55] (their proof holds also for the grand canonical ensemble). The normal pressure can be easily obtained from $p_\perp = k_B T \rho(\pm L/2)$ (k_B: Boltzmann constant, $\rho(\pm L/2)$: contact value of the fluid density profile at pore walls). By using thus obtained $p_\perp$, we obtain the differential surface tension straightforwardly from eq. (7).

Since the differential surface tension is ensemble-independent, we can also calculate it with the mechanical definition, i.e., eq. (1), in a canonical ensemble. The test-volume and test-area methods [39-41] are based on this principle. We used also these methods to calculate the averaged values of the two components of pressure tensor in order to compare γ from the canonical ensemble with that obtained from the grand canonical ensemble to evidence effectively its ensemble-independence.

C. Calculation of integral surface tension, $\hat{\gamma}_G$

In order to show clearly our procedure for calculating $\hat{\gamma}_G$, it is useful to recall that Gibbs free energy is a first-order homogeneous function of N and $\mathcal{A}$. i.e.,

$$G(T, p_\perp, \lambda N, \lambda \mathcal{A}) = \lambda G(T, p_\perp, N, \mathcal{A}). \quad (8)$$

This leads immediately to

$$G(T, p_\perp, N, \mathcal{A}) = \mu N + \gamma \mathcal{A}, \quad (9)$$

where μ is the chemical potential of the confined fluid. We first calculate the chemical potential with Widom's test particle method [56] and γ with the help of its mechanical definition and the test-volume method for the components of pressure tensor [39] in canonical ensemble. Since both μ and γ are differential intensive variables, thus ensemble-independent, we can use them to calculate Gibbs free energy by using eq. (9). Once G is determined, we obtain readily the integral surface tension, $\hat{\gamma}_G$, from its definition, i.e., eq. (4) with μ^{bulk} being the chemical potential of the corresponding bulk fluid at the same *T* with a pressure equal to $p_\perp$. We use Carnahan-Stirling equation for calculating μ^{bulk} since it gives essentially the exact result for a bulk hard sphere fluid.

III. Results

In order to enhance their visual perception, all the results shown in the main text are presented in form of curves. However, the numerical data given in tables can facilitate their use by other researchers who wish to compare their own results with ours. Such tables along with detailed computational parameters and conditions are presented as Supplementary Material (SM).

Now, we present first the simulation evidence for the distinct integral and differential surface tensions. Fig. 2 show the results for $\hat{\gamma}_\Omega$ and γ as a function of chemical potential which are obtained

in a grand canonical ensemble by using respectively the methods described in Sec. II-A and Sec. II-B. We see clearly that for narrow pores, γ (continuous curves) is different from $\hat{\gamma}_\Omega$ (dash-dot curves). The differential surface tension changes significantly with the pore width while the modification of the integral surface tension with the pore width is moderate. We see also that the difference between $\hat{\gamma}_\Omega$ and γ increases with the chemical potential. So, it is easier to detect this difference at high fluid densities. For the system studied here, the largest difference between $\hat{\gamma}_\Omega$ and γ is found for the pore width, $L = 1.5\sigma$ (see the red curves in Fig. 2).

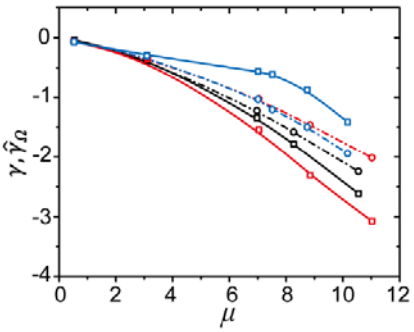

FIG.2. Results evidencing distinct integral and differential surface tensions from grand canonical transition matrix Monte Carlo simulation. $\hat{\gamma}_\Omega$: symbols and dash-dot lines; γ: symbols and continuous lines. Symbols are original simulation data and lines are fittings with a third-order polynomial. Three pore widths are considered: $L = 0.25\sigma$ (black), $L = 1.5\sigma$ (red), $L = 2.0\sigma$ (blue). Details about computational conditions are given in Supplementary Material (SM).

We have recalled above that the integral surface tension, $\hat{\gamma}_\Omega$, satisfies a generalized Gibbs adsorption equation, i.e., eq. (5). From our grand canonical ensemble simulations, we can readily calculate the adsorption, i.e., the right-hand-side (RHS) of eq. (5). The results of $\hat{\gamma}_\Omega$ as a function of μ allow for determining the derivative on the left-hand-side of eq. (5). In order to calculate accurately the derivative, the simulation data in Fig. 2 are fit to smooth curves (dash-dot lines). The thus obtained derivatives of $\hat{\gamma}_\Omega$ with respect to μ are presented in Fig. 3 as lines while the simulation results for $-\Gamma$ are shown as symbols. The good agreement between the lines and the symbols shown in Fig. 3 evidences the validity of the generalized Gibbs adsorption equation.

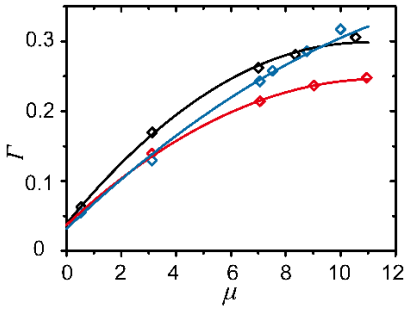

FIG.3. Corroboration of adsorption equation satisfied by the integral surface tension, $\hat{\gamma}_\Omega$. Values of $-(\partial\hat{\gamma}_\Omega/\partial\mu)_{T,L}$: Continuous lines; Adsorption, Γ: Symbols. Three pore widths are considered: $L = 0.25\sigma$ (black), $L = 1.5\sigma$ (red), $L = 2.0\sigma$ (blue). Details about computational conditions are given in SM.

Hill first point out that the ensemble-dependence is one salient feature of the thermodynamics of small systems [1,2]. The recent work of W. Dong has further clarified that only integral intensive variables are ensemble-dependent while the differential intensive variables are not [23]. In Sec. II-B, we described the respective the procedure to calculate γ in a grand canonical ensemble, as well as that in a canonical ensemble. In addition to the results of γ obtained in a grand canonical ensemble (those in Fig. 2), we also calculated γ in a canonical ensemble with the help of its mechanical definition and the test-volume method to calculate the averaged components of pressure tensor. These results of γ from different ensembles are presented in Fig. 4 (continuous curves for μVT-ensemble and symbols for *NVT*-ensemble). The good agreement between the results from different ensembles confirms well the ensemble-independence of the differential surface tension.

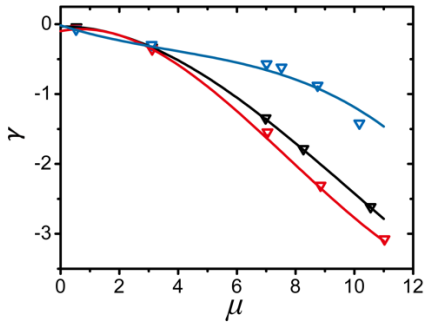

FIG. 4. Ensemble-independence of differential surface tension evidenced by comparing the μVT-ensemble simulation results (continuous curves) and those from *NVT*-ensemble (symbols). Three pore widths are considered: $L = 0.25\sigma$ (black), $L = 1.5\sigma$ (red), $L = 2.0\sigma$ (blue). Details about computational conditions are given in SI.

In Sec. II-C, the method for calculating Gibbs free energy with our simulation data is described. We used again Carnahan-Stirling equation to calculate the chemical potential of a bulk hard sphere fluid, μ^{bulk}, at a pressure equal to the value of the normal pressure in the confined fluid. Then, eq. (4) allows for calculating straightforwardly $\hat{\gamma}_G$. The results for $\hat{\gamma}_G$ as a function of $p_\perp$ are presented in Fig. 5 along with the differential surface tension. We see that $\hat{\gamma}_G$ is also different from γ and their difference is even more pronounced than that between $\hat{\gamma}_\Omega$ and γ. Concerning the influence of the pore width on γ and $\hat{\gamma}_G$, Fig. 5 shows that $\hat{\gamma}_G$ changes slightly when the pore width is modified while the differential surface tension is much more sensitive to the change of the pore width as what is already observed from the results given in Fig. 2.

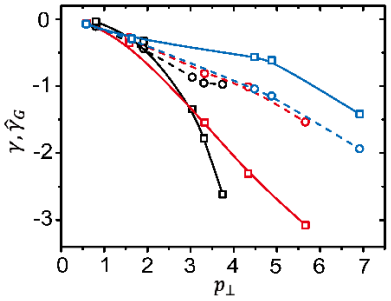

FIG. 5. Integral surface tension defined from Gibbs free energy, $\hat{\gamma}_G$ (symbols being simulation data and dash lines for guiding the eye) as a function of normal pressure, compared to differential surface tension, γ (symbols being simulation data and full lines for guiding the eye). Three pore widths are considered: $L = 0.5\sigma$ (black), $L = 1.0\sigma$ (red), $L = 1.5\sigma$ (blue).

Finally, the ensemble dependence of the integral surface tensions is evidenced by the results presented in Fig. 6, which shows clearly that $\hat{\gamma}_G \neq \hat{\gamma}_\Omega$. From Fig. 6, one can see that for $L = 2.0\sigma$, the curve of $\hat{\gamma}_G$ overlaps nearly that of $\hat{\gamma}_\Omega$, so the ensemble-dependence of the integral surface tension becomes negligible for pores with a width larger than 2.0σ. However, a pronounced ensemble-dependence is observed for strong confinements, $L < 2.0\sigma$.

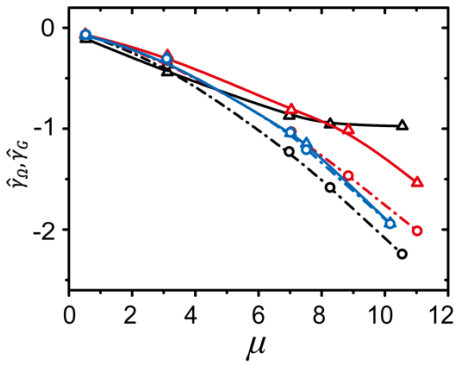

FIG. 6. Ensemble-dependence of integral surface tensions. Integral surface tension defined from grand potential, $\hat{\gamma}_\Omega$: symbols being simulation data and dash-dot lines given by fittings with a third-order polynomial; Integral surface tension defined from Gibbs free energy, $\hat{\gamma}_G$: symbols being simulation data and full lines for guiding the eye. Three pore widths are considered: $L = 0.25\sigma$ (black), $L = 1.5\sigma$ (red), $L = 2.0\sigma$ (blue).

IV. Discussion

The results of the present study provide the simulation evidences for the general validation of the concept of distinct differential and integral surface tensions [22,23], i.e., $\gamma \neq \hat{\gamma}_\Omega \neq \hat{\gamma}_G$, when the size of an interfacial system shrinks down in the direction normal to the interface. The mechanical definition and the differential thermodynamic definition of surface tension are ensemble-independent and give the same result, i.e. $\gamma = \gamma^{\text{mech}}$. But the integral surface tensions are ensemble-dependent, e.g., $\hat{\gamma}_\Omega \neq \hat{\gamma}_G$ in cases of strong confinement. In contrast to Hill's nanothermodynamics, the alternative approach proposed recently [22,23] focuses on a single small system without resorting to the artifice of replica proposed by Hill. Now, a physically-appealing measure for quantifying a system's smallness emerges as well. In fact, down to which size, a system can be qualified as a small one? Before answering this question, it is to note that the absolute value of the size does not always provide a suitable answer to such a question. For the system considered in this work, it is the pore size compared to the fluid-particle size that really matters. A more quantitative characterization of different degrees of smallness can be formulated according to successive modifications of the thermodynamic properties due to the size decrease. For the prototype system considered in this work, when the pore width becomes smaller, one finds first $p_\perp \neq \hat{p}$ (differential pressure: $p_\perp = -(\partial\Omega/\partial V)_{T,\mu,\mathcal{A}}$, integral pressure: $\hat{p} = -\Omega/V$) and $\mu \neq \hat{\mu}$ (differential chemical potential: $\mu = (\partial G/\partial N)_{T,p_\perp,\mathcal{A}}$, integral chemical potential: $\hat{\mu} = G/N$). Further decreasing the pore width leads to $\gamma \neq \hat{\gamma}_\Omega \neq \hat{\gamma}_G$ in addition

to $p_\perp \neq \hat{p},\ \mu \neq \hat{\mu}$.

The new concept of differential and integral surface tensions improves not only our understanding of the thermodynamic properties of small systems but also our knowledge about various simulation methods for determining surface tensions. Up to now, it is believed that all the simulation methods give the same result for surface tension. However, this is no longer true when the surface contribution becomes dominant in the thermodynamic potential. Under such conditions, the methods based on the differential definition or the mechanical definition do not give the same result as those based on the integral definition of surface tension. For example, the first category, including the methods based on pressure tensor [36,37] or the test area method [39-41], gives the differential surface tension while the second category, including the thermodynamic integration method [43] and that base on integrating Gibbs adsorption equation [46,47], gives the integral surface tension. When the methods of the second category are used, particular attention has to be payed also to the ensemble-dependence of the obtained results. The general validity of the approach proposed recently by W. Dong [22,23] is demonstrated by the simulations reported in this work. We hope this will provide an impetus to the investigations for its experimental validation. We also hope that the present work can motivate further theoretical investigations. Intensives variables, like pressure and chemical potential, play an important role for describing phase equilibria. It is not yet clear whether it is the differential or the integral intensive variables that determine the phase equilibria in small systems. Advance in clarifying such open issues will certainly benefit the development of nanoscience and nanotechnology.

Although the hard sphere fluid is a quite simple model for fluids, it is now well-known that it is capable of describing quite well the properties of many colloid systems. Moreover, granular gases resemble in many aspects to a hard sphere fluid although their motion is not a thermal one but driven by the vibration of the plateau on which they are placed. Recently, some experiments with granular gases have provided very interesting results for corroborating some theoretical predictions of stochastic thermodynamics [57-60]. One can wonder how a granular gas which is a macroscopic system can be used to test the predictions of the nanoscale thermodynamics. In fact, if a granular gas can be confined in a slit pore of a width in the range of a few diameters of a granular, the system is under the strong confinement conditions. Such a system should manifest the same behaviors as those observed from our simulations. As already pointed out above, the really relevant physical measure of smallness is not the absolute size but the pore width compared to the fluid-particle size. Under the condition of strong

confinement, the fluid adsorption near one pore wall affects that on the other wall. Thus, there is no long a clear distinction of bulk and interface regions in such a system, the characteristic thermodynamic behaviors of small systems will manifest themselves. The strategy described above should allow for devising possible experimental investigations with granular gases and our simulation results will be certainly useful to help finding the suitable experimental conditions.

References

1. T. L. Hill, Thermodynamics of small systems. J. Chem. Phys. **36**, 3182 (1962).

2. T. L. Hill, *Thermodynamics of small systems, Part 1 and 2*, Benjamin, New York, (1963).

3. R. V. Chamberlin, Mean-field cluster model for the critical behaviour of ferromagnetts. Nature, **408**, 337 (2000).

4. T. L. Hill, Perspective: Nanothermodynamics. Nano Lett. **1**, 111 (2001).

5. D. Bedeaux, S. Kjelstrup and S. K. Schnell, *Nanothermodynamics. Theory and Applications*, World Scientific, Singapore, (2024).

6. B. A. Strom, J. M. Simon, S. K. Schnell, S. Kjelstrup, J. He, and D. Bedeaux, Size and shape effects on the thermodynamic properties of nanoscale volumes of water. PCCP **19**, 9016 (2017).

7. N. Dawass, P. Kruger, S. K. Schnell, D. Bedeaux, S. Kjelstrup, J. M. Simon and T. J. H. Vlugt, Finite-size effects of Kirkwood–Buff integrals from molecular simulations. Mol. Simulation **44**, 599-612 (2018).

8. D. Bedeaux and S. Kjelstrup, Hill's nano-thermodynamics is equivalent with Gibbs' thermodynamics for surfaces of constant curvatures. Chem. Phys. Lett. **707**, 40-43 (2018).

9. O. Galteland, D. Bedeaux, B. Hafskjold and S. Kjelstrup, Pressures inside a nano-porous medium. The case of a single phase fluid. Frontiers in Physics **7**, 60 (2019).

10. M. Erdos, O. Galteland, D. Bedeaux, S. Kjelstrup, O. A. Moultos and T. J. H. Vlugt, Gibbs ensemble Monte Carlo simulation of fluids in confinement: Relation between the differential and integral pressures. Nanomaterials **10**, 293 (2020).

11. M. T. Rauter, O. Galteland, M. Erdos, O. A. Moultos, T. J. H. Vlugt, S. K. Schnell, D. Bedeaux and S. Kjelstrup, Two-phase equilibrium conditions in nanopores. Nanomaterials **10**, 608 (2020).

12. B. A. Strom, J. Y. He, D. Bedeaux, and S. Kjelstrup, When thermodynamic properties of adsorbed films depend on size: Fundamental theory and case study. Nanomaterials **10**, 1691 (2020).

13. E. Bering, D. Bedeaux, S. Kjelstrup, A. S. de Wijn, I. Latella, and J. M. Rubi, A Legendre–Fenchel

transform for molecular stretching energies. Nanomaterials **10**, 2355 (2020).

14. O. Galteland, D. Bedeaux, and S. Kjelstrup, Nanothermodynamic description and molecular simulation of a single-phase fluid in a slit pore. Nanomaterials **11**, 165 (2021).

15. O. Galteland, E. Bering, K. Kristiansen, D. Bedeaux and S. Kjelstrup, Legendre-Fenchel transforms capture layering transitions in porous media. Nanoscale Adv. **4**, 2660 (2022).

16. J. M. Simon, P. Kruger, S. K. Schnell, T. J. H. Vlugt, S. Kjeslstrup and D. Bedeaux, Kirkwood–Buff integrals: From fluctuations in finite volumes to the thermodynamic limit. J. Chem. Phys. **157**, 130901 (2022).

17. Z. Lu and H. Qian, Emergence and breaking of duality symmetry in generalized fundamental thermodynamic relations. Phys. Rev. Lett. **128**, 150603 (2022).

18. R. de Miguel and J. M. Rubi, Finite systems in a heat bath: spectrum perturbations and thermodynamics. J. Phys. Chem. B **120**, 9180 (2016).

19. R. de Miguel and J. M. Rubi, Thermodynamics far from the thermodynamic limit. J. Phys. Chem. B **121**, 10429 (2017).

20. Yu. K. Tovbin, Lower size boundary for the applicability of thermodynamics. Russ. J. Phys. Chem. A **86**, 1356 (2012).

21. Yu. K. Tovbin, *Small systems and fundamentals of thermodynamics*, CRC Press, Taylor & Francis Group, Boca Raton, London, New York (2019).

22. W. Dong, Thermodynamics of interfaces extended to nanoscales by introducing integral and differential surface tensions. PNAS **118**, e2019873118 (2021).

23. W. Dong, Nanoscale thermodynamics needs the concept of a disjoining chemical potential. Nature Communications **14**, 1824 (2023).

24. P. S. de Laplace, *Traité de Mécanique Céleste. Tome IV, Supplément au dixième livre, Sur l'Action Capillaire*, Courcier Paris (1806) ; *Supplément à la Théorie de l'Action Capillaire* (1807).

25. T. Young, An essay on the cohesion of fluids. Phil. Trans. Roy. Soc. **95**, 65 (1805).

26. J. W. Gibbs, *The Collected Works of J. W. Gibbs, Volume 1. Thermodynamics*, Longmans, Green and Co., New York, London, Toronto, (1928).

27. J. G. Kirkwood and F. P. Buff, The statistical mechanical theory of surface tension. J. Chem. Phys. **17**, 338 (1949).

28. J. H. Irving and J. G. Kirkwood, The statistical mechanical theory of transport processes. IV. The

372 equations of hydrodynamics. J. Chem. Phys. **18**, 817 (1950).
373 29. S. Ono and S. Kondo, P_{134}-P_{280} in *Encyclopedia of Physics*, *Volume X*, edited by S. Flügge,
374 Springer-Verlag, Berlin, Götingen, Heidelberg, (1960).
375 30. J. S. Rowlinson and B. Widom, *Molecular Theory of Capilarity*, Oxford University Press, New
376 York, (1980).
377 31. A. Ghoufi, P. Malfreyt and D. J. Tildesley, Computer modelling of the surface tension of the gas-
378 liquid and liquid-liquid interface. Chem. Soc. Rev. **45**, 1387 (2016).
379 32. A. Ghoufi, Surface free energy calculation of the solid-fluid interfaces from molecular simulation.
380 AIP Advances **14**, 045116 (2024).
381 33. A. Ghoufi and P. Malfreyt, Calculation of the surface tension and pressure components from a non-
382 exponential perturbation method of the thermodynamic route. J. Chem. Phys. **136**, 024104 (2012).
383 34. A. Ghoufi, F. Goujon, V. Lachet and P. Malfreyt, Mutiple histogram reweighting method for the
384 surface tension calculation. J. Chem. Phys. **128**, 154718 (2008).
385 35. J. R. Hendeson and F. van Swol, On the interface between a fluid and a planar wall: theory and
386 simulations of a hard sphere fluid at a hard wall. Mol. Phys. **51**, 991 (1984).
387 36. B. D. Todd, D. J. Evans and P. J. Davis, Pressure tensor for inhomogeneous fluids. Phys. Rev. E
388 **52**, 1627 (1995).
389 37. F. Varnik, J. Baschnagel and K. Binder, Molecular dynamics results on the pressure tensor of
390 polymer films. J. Chem. Phys. **113**, 4444 (2000).
391 38. K. Fujiwara and M. Shibahara, Local pressure components and interfacial tension at a liquid-solid
392 interface obtained by the perturbative method in the Lennard-Jones system. J. Chem. Phys. **141**,
393 034707 (2014).
394 39. E. de Miguel and G. Jackson, Detailed examination of the calculation of the pressure in
395 simulations of systems with discontinuous interactions from the mechanical and thermodynamic
396 perspectives. Mol. Phys. **104**, 3717 (2006).
397 40. G. J. Gloor, G. Jackson, F. J. Blas and E. de Miguel, Test-area simulation method for the direct
398 determination of the interfacial tension of systems with continuous or discontinuous potentials. J.
399 Chem. Phys. **123**, 134703 (2005).
400 41. J. M. Miguez, M. M. Piñeiro, A. I. Moreno-Ventas Bravo and F. J. Blas, On interfacial tension
401 calculation from the test-area methodology in the grand canonical ensemble. J. Chem. Phys. **136**,

114707 (2012).
42. L. G. MacDowell and P. Bryk, Direct calculation of interfacial tensions from computer simulation: Results for freely jointed tangent hard sphere chains. Phys. Rev. E **75**, 061609 (2007).
43. M. Heni and H. Löwen, Interfacial free energy of hard-sphere fluids and solids near a hard wall. Phys. Rev. E **60**, 7057 (1999).
44. J. Mittal, J. R. Errington, and T. M. Truskett, Does confining the hard-sphere fluid between hard walls change its average properties? J. Chem. Phys. **126**, 244708 (2007).
45. R. Benjamin and J. Horbach, Wall-liquid and wall-crystal interfacial free energies via thermodynamic integration: A molecular dynamics simulation study. J. Chem. Phys. **137**, 044707 (2012).
46. B. B. Laird and R. L. Davidchack, Calculation of the interfacial free energy of a fluid at a static wall by Gibbs–Cahn integration. J. Chem. Phys. **132**, 204101 (2010).
47. R. L. Davidchack B. B. Laird and R. Roth, Parameterising the surface free energy and excess adsorption of a hard-sphere fluid at a planar hard wall. Mol. Phys. **113**, 1091 (2015).
48. N. Wu, X. Ji, R. An, C. Liu and X. Lu, Generalized Gibbs free energy of confined nanoparticles. AIChE Journal **63**, 4595 (2017).
49. Q. Gao, Y. Zhang, S. Xu, A. Laaksonen, Y. Zhu, X. Ji and X. Lu, Physicolchemical properties and structure of fluid at nano-/micro-interface: Progress in simulation and experimental study. Green Energy & Environment **5**, 274 (2020).
50. J. W. Cahn, Free energy of a nonuniform system. II. Thermodynamic basis. J. Chem. Phys. **30**, 1121 (1959).
51. J. R. Errington, Evaluating surface tension using grand canonical transition-matrix Monte Carlo simulation and finite-size scaling. Phys. Rev. E **67**, 012102 (2003).
52. J. R. Errington, Direct calculation of liquid–vapor phase equilibria from transition matrix Monte Carlo simulation. J. Chem. Phys. **118**, 9915 (2003).
53. B. V. Derjaguin, Y. I. Rabinovich and N. V. Churaev, Direct measurement of molecular forces. Nature **272**, 313-318 (1978).
54. B. V. Derjaguin, N. V. Churaev and V. M. Muller, *Surface forces*. Springer Science+Business Media, LLC, (1987).
55. W. Dong, T. Franosch and R. Schilling, Thermodynamics, statistical mechanics and the vanishing

pore width limit of confined fluids. Communications Physics **6**, 161 (2023).

56. B. Widom, Some topics in the theory of fluids. J. Chem. Phys. **39,** 2808 (1963).

57. K. Cheng, J.-Q. Dong, W.-H. Han, F. Liu, and L. Huang. Infima statistics of entropy production in an underdamped Brownian motor. Phys. Rev. E. **102**, 06 (2020).

58. K. Cheng, J.-Q. Dong, L. Huang and L. Yang. Cover-time distribution of random processes in granular gases. Phys. Rev. E. **98**, 04 (2018).

59. J.-Q. Dong, W.-H. Han, Y. Wang, X.-S. Chen, and L. Huang, Universal Cover-Time Distribution of Heterogeneous Random Walks, Phys. Rev. E **107**, 024128 (2023).

60. W. H. Han, K. Cheng, X. N. Liu, J. Q. Dong, X. S. Chen and L. Huang, Universal Cover-Time Distribution of Random Motion in Bounded Granular Gases, Chaos, **33** 023127 (2023).

Acknowledgements

We thank the financial support of the National Natural Science Foundation of China (N°. 22178072) and the Pôle Scientifique de Modélisation Numérique of Ecole Normale Supérieure de Lyon for computational resources. SLZ acknowledges the financial support from the Guangxi Science and Technology Major Program (No. AA23073019). HRJ is grateful to the financial support of the French Government through an Eiffel scholarship, that of China Scholarship Council through a CSC scholarship (project No. 202106740013) and that from le Conseil Régional Auvergne-Rhône-Alpes (France).